The Rate of Movement of the Topochemical Interface During Gas-Solid Reactions

R. P. KING AND C. P. BROWN

The rate of recession of the topochemical interface between a porous core and the product layer is shown to be given by

$$\frac{dr_c}{dt} = \frac{R(r_c)}{\left.\frac{dC_s}{dr}\right|_{r_c}}$$

where r_c is radial position of the interface, $R(r_c)$ the rate of the chemical reaction at the interface and $(dC_s/dr)|_{r_c}$ is the gradient of concentration profile of solid reactant in the porous core at the interface. The integration of the above equation can sometimes be achieved analytically but can always be done numerically for even highly complex reaction mechanisms. The equation correctly reduces to previously known solutions when the inner core is impervious to gas diffusion. The utility of the equation is demonstrated by applying it to the industrially important multistage reduction process $Mn_3O_4 \rightarrow MnO \rightarrow Mn$. The predictions from the theoretical model are compared successfully with experimental data for this reaction.

THE topochemical nature of several important metallurgical gas-solid reactions has been demonstrated in many studies. The development of effective mathematical models for the quantitative analysis of such gas-solid reactions has received a great deal of attention in the literature and suitable mathematical models have been developed for the description of many practical situations. Much of the theoretical work has been directed towards the problem of developing simplified models under conditions where only one of the various diffusional or chemical kinetic processes control the overall rate of the process. Such simplifications, while often having the advantage of simplicity, are not always appropriate since mixed control and the transition from one control mechanism to another are frequently met. A common feature of all topochemical models is that a definite interface exists which marks the closest distance from the particle surface that a particular solid reactant is found. Such an interface recedes towards the center of the particle as the reaction proceeds finally vanishing at the center at a time which marks the completion of the conversion of the particular solid reactant. Sometimes the interface is very sharp, with the reactant concentration falling very rapidly to zero over a short distance. This occurs when the reaction is localized at or very close to the interface. In other circumstances the reaction zone is diffuse and the concentration of solid reactant falls gradually outwards until it become zero at the topochemical interface. In these diffuse zones the gaseous reactant penetrates into the incompletely reacted solid by diffusion so that chemical reaction and diffusion occur simultaneously.

R. P. KING is Professor of Extractive Metallurgical Engineering, Department of Metallurgy, University of the Witwatersrand, Johannesburg, South Africa. C. P. BROWN, formerly Student in Department of Metallurgy, University of Strathclyde, Scotland, is now with Westland Helicopters, Yeovil, England.

Manuscript submitted May 3, 1979.

The position of the topochemical interface is a particularly important parameter because the instantaneous rate of conversion in the reacting particle and the total conversion within the particle can be uniquely related to interface position. This is important whenever it is required to calculate the performance of a fixed, moving or fluidized bed reactor in which the solid particles are being converted. Moving bed reactors are models for such important industrial equipment as rotary kilns, the shaft of the blast furnace and the upper section of the submerged arc furnace. Spitzer *et al*,[1] Ishida and Wen[2] and Yagi *et al*[3] have considered these models and have emphasized the importance of the topochemical interface as the defining parameter for both the instantaneous conversion and rate of conversion of the solid. Szekely *et al*[4] have also used the core radius within an individual grain in a pellet as an indicator of the grain conversion. With the exception of Spitzer *et al*, each of the above authors have considered only the impervious-core model for the individual particles. We shall be particularly concerned with porous-core models in this paper.

Various approximate[1,5-8] expressions have been reported in the literature for the velocity of the interface in the porous-core situation and these must always be used with caution if serious errors are to be avoided. An exact general expression is developed here which can be used at any topochemical interface no matter what particular model is used for the description of the reaction process.

A GENERAL EQUATION FOR THE VELOCITY OF THE INTERFACE

It is assumed that the chemical reaction takes place on the surface of the solid and that the solid is itself a reactant. Another reactant must be present and is transported to the reaction site by an appropriate

ISSN 0360-2141/80/1211-0585$00.75/0

diffusion mechanism. The products of reaction may be solid (in which case they remain at the reaction site) or gas in which case they are transported away from the reaction site. If the solid product remains in position it must be sufficiently porous to allow the continued access of reactant to the reaction site. Thus the reactant gas diffuses into the solid through a layer of reaction product.

An essential second assumption is that the activity of the solid reactant is independent of its concentration in the solid phase and the rate of the chemical reaction is independent of that concentration. This means in particular that the solid reactant can be completely reacted at any point in a particle and its concentration reduced to zero. It is this behavior that produces the well defined topochemical interface within the particle and the validity of the assumption has been directly confirmed by several reported experiments (Nabi and Lu,[9] Turkdogan and Vinters,[10] Mantri *et al*,[6] Takahashi *et al*[11]).

Two distinct situations must be considered: those in which the core is sufficiently porous to permit the diffusion of reactant gases and thus reaction to take place within the core and those situations in which the core is impervious to reactant gases and in which all reaction is localized at the interface between the unreacted solid in the core and the product layer.

Porous Core Models

As reaction proceeds, the interface between the reactant and product layers recedes. The rate of recession is determined by the concentration gradient of the solid reactant within the core and the concentration of diffusing reactant at the interface. The situation at the interface is shown schematically in Fig. 1.

The concentration profiles of diffusing species and solid reactant are illustrated. The profiles shown by means of broken lines occur a short time, Δt after those represented by the full lines. The interface recedes a distance Δr_c during this time interval. This distance is defined by the change ΔC_s that is required to bring the solid concentration to zero at the new interface after time Δt. ΔC_s is related to Δr_c by the slope of the solid concentration profile at the interface.

$$\frac{\Delta C_s}{\Delta r_c} \simeq \left.\frac{dC_s}{dr}\right|_{r=r_c} \qquad [1]$$

On the other hand ΔC_s is also related to the rate of reaction at the interface

$$\Delta C_s \simeq R(r_c)\Delta t \qquad [2]$$

where $R(r_c)$ is the rate of the chemical reaction in mols solid reactant/m^{3}s at the interface.

Equations [1] and [2] combine to give

$$\frac{\Delta r_c}{\Delta t} \simeq \frac{R(r_c)}{\left.\frac{dC_s}{dr}\right|_{r=r_c}} \qquad [3]$$

In the limit as $\Delta t \rightarrow 0$ Eq. [3] becomes exact and the velocity of the interface is given by

$$\frac{dr_c}{dt} = \frac{R(r_c)}{\left.\frac{dC_s}{dr}\right|_{r=r_c}} \qquad [4]^*$$

*A referee has pointed out Eq. [4] results directly from an application of the chain rule

$$R(r_c) = \left.\frac{dC_s}{dt}\right|_{r=r_c} = \left(\frac{dC_s}{dr}\frac{dr}{dt}\right)_{r=r_c}$$

$$= \left.\frac{dr_c}{dt}\frac{dC_s}{dr}\right|_{r=r_c}$$

In Eq. [4] the rate of the chemical reaction at the interface $R(r_c)$ is defined by the relationship between the reaction rate and the mole fractions of the reactant and product gases at the interface. These partial pressures are in turn determined by the diffusional processes through the porous product layer and the porous core.

We show later by means of an example how Eq. [4] can be used in practical cases but first we show that it does not conflict with known solutions that have already appeared in the literature.

The simplest problem to which Eq. [4] can be applied is the case of a single reaction taking place in a spherical

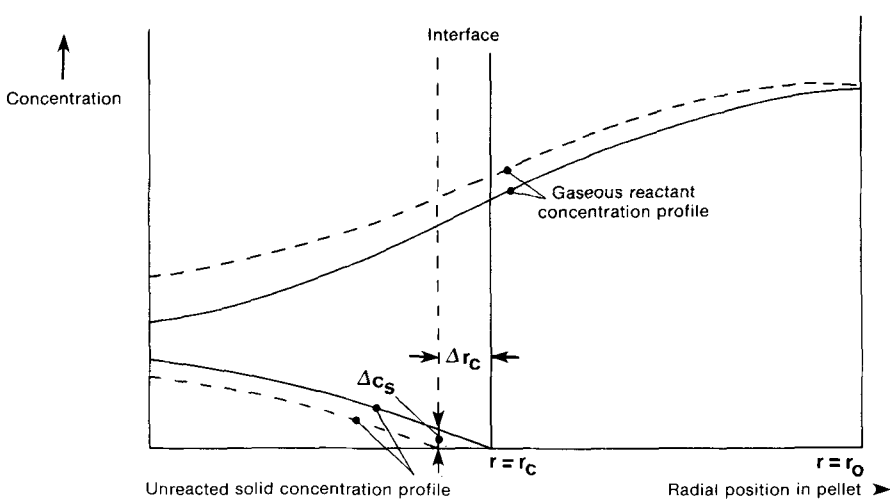

Fig. 1—Concentration profiles inside a porous reacting pellet. Broken lines represent profiles a short time after the profile shown by full lines.

porous particle. This model has been completely solved by Ishida and Wen[12] and it is useful to use their solution to show how Eq. [4] can be used and to confirm that it produces the same result.

Ishida and Wen have shown that, when the reaction rate is a linear function of a gas-phase composition,

$$R(r_c) = \frac{R_b}{\theta} \qquad [5]$$

where R_b is the reaction rate at a composition equivalent to the bulk gas phase and θ is a parameter accounting for the resistance of any gas film on the outer surface of the particle, the resistance of the solid product layer and the distributed reaction in the porous core,

$$\theta = 1 + \frac{D'_e}{D_e}(1 - \bar{\xi} + \bar{\xi}/N_{Sh})(\phi\bar{\xi}\coth(\phi\bar{\xi}) - 1). \qquad [6]$$

ξ is the dimensionless core radius, r_c/r_o, D'_e is the effective diffusivity of the reductant in the porous core, D_e that in the product layer and N_{Sh} is the Sherwood number $k_g r_o/D_e$ for mass transfer through the boundary layer. ϕ is the kinetic-diffusion parameter for the porous core defined by

$$\phi = \left(\frac{s\rho k(1 + K)}{D'_e K}\right)^{1/2} r_o. \qquad [7]$$

r_o is the particle radius, s the pore surface area per unit mass of solid and ρ is the solid bulk density of the solid. K is the equilibrium constant and we have assumed a reaction of the type

$$A(s) + B(g) = C(s) + D(g) \qquad [8]$$

having a rate law

$$R = s\rho kC(y_B - y_D/K) \qquad [9]$$

Ishida and Wen also found the solid reactant concentration profile within the porous core to be given by

$$\frac{C_s}{C_s^o} = 1 - \frac{\bar{\xi}\sinh(\phi\xi)}{\xi\sinh(\phi\bar{\xi})}. \qquad [10]$$

Substitution of Eqs. [5] and [10] into Eq. [4] gives

$$\frac{dr_c}{dt} = -\frac{r_c R_b}{C_s^o\theta(\phi\bar{\xi}\coth(\phi\bar{\xi}) - 1)}. \qquad [11]$$

Equation [11] is identical to that found by Ishida and Wen via an equivalent integral equation.

Impervious Core Models

A particularly important limiting case occurs when the reacting core is impervious to the reductant. This occurs under three important conditions: when the solid reactant is so well consolidated that diffusion of even gaseous reductant is very slow, when the reducing agent can diffuse only in one of the solid products of reaction or when the chemical reaction is very fast in comparison to the diffusion process. The first situation was encountered by Nabi and Lu,[9] for example, who studied the reduction of dense hematite by hydrogen. The second occurs when reactant diffusing through the product layer is not the gaseous reductant but oxygen ions (Lien *et al*[13]) or Fe^{3+} ions in Wustite (von Bogdandy and Engell[14]). Another very important example occurs when the final stages of reduction requires a thermodynamically more powerful reducing agent than CO or H_2 which are normally active in industrial reduction processes. Examples are the reduction of MnO in the final stages of the reduction of the commercially important manganese ores and the reduction of Cr_2O_3. In both cases, the thermodynamic equilibrium is so unfavorable that the reduction can only be effected at an appreciable rate by carbon or an appropriate metal carbide. The rate of diffusion of carbon in the oxide is completely negligible although its movement through the metallized product layer as the appropriate carbide is sufficiently rapid to maintain adequate rates of reduction for practical applications (Barcza *et al*[15] Grimsley *et al*[16]).

Under these conditions all the reaction is concentrated at the surface of the shrinking core and the so-called shrinking core models are appropriate. Simple models of this type date back to the work of Ginstling and Brounstein (1950).[16] The entire mathematical model is usually derived from the basis that the chemical reaction is concentrated entirely at the interface between the unreacted reactant and the product layer (Nabi and Lu,[9] Scrivner and Manning[18]). However, the equations can be obtained as an appropriate limit of those for the porous core models and in this way the effect of individual processes can be more easily seen. Equation [7] indicates that any one of three parameters may give rise to a concentration of the chemical reaction at the interface: D'_e very small, k very large or K very small. These correspond to the situations referred to at the beginning of this section. Each of these parameters influence the diffusion-kinetic parameter, ϕ, of the model and from Eq. [7] it is easy to see that the impervious core model results when ϕ tends to infinity. However, the limit must be approached in such a way that the group

$$\kappa = \left(\frac{D'_e k s\rho K}{(K + 1)}\right)^{1/2} \qquad [12]$$

remains finite. κ is the specific rate constant for the surface reaction. That is, the rate of reaction in mol/s m^2 of core surface area is given by

$$R_s = C\kappa(y_{Bc} - y_{Dc}/K) \qquad [13]$$

Equation [12] shows explicitly the relationship between κ and the various physical constants.

The rate of movement of the core surface is given by Eq. [11] as

$$\frac{dr_c}{dt} = \lim_{\substack{\phi\to\infty \\ \kappa \text{ finite}}}\left(-\frac{r_c R_b}{C_s^o\theta(\phi\bar{\xi}\coth(\phi\bar{\xi}) - 1)}\right) \qquad [14]$$

$$= \lim_{\substack{\phi\to\infty \\ \kappa \text{ finite}}}\left(-\frac{r_c s\rho kC(y_{B,b} - y_{D,b}/K)}{C_s^o\phi\bar{\xi}(1 + (\phi\bar{\xi}D'_e/D_e)(1 - \bar{\xi} + \bar{\xi}/N_{Sh}))}\right) \qquad [15]$$

$$= -\frac{(C/C_s^o)(y_{B,b} - y_{D,b}/K)}{\frac{1}{\kappa} + \frac{1+K}{D_e K}\left(1 - \frac{r_c}{r_o} + \frac{r_c}{r_o N_{sh}}\right) r_c} \quad [16]$$

which is identical to the expression derived by Scrivner and Manning[18] from the assumption that the core was impervious confirming that Eq. [4] is consistent with the usual assumptions.

EXTENSION OF THE BASIC MODELS FOR MULTISTAGE REDUCTIONS

The simple formulations presented above must be extended if the reduction passes through several stages such as, for example, the hematite, magnetite, Wustite, iron sequence for iron ores or the Mn_2O_3, Mn_3O_4, MnO, Mn sequence for manganese ores. Experimental evidence (Turkdogan and Vinters,[10] Grimsley *et al*[16]) suggests that such sequences give rise to a layered structure within the particle with the layers separated by diffuse interfaces. The topochemical nature of the process is maintained because each successive oxide is completely depleted at some point in the pellet. Consequently an interface for each oxide can be defined as the radius at which its concentration becomes zero. The overall reaction proceeds in stages as the various interfaces are developed and then recede towards the interior of the particle.

The reduction of Mn_3O_4 by carbon is an interesting example of the basic models. CO is generated at points of contact between the oxide and carbon particles by the reaction $Mn_3O_4 + C = 3MnO + CO$. Grimsley *et al*[16] demonstrated that this reaction was not rate limiting by showing that the rate of reduction (at least to MnO) was not affected by changing the gas atmosphere from argon to CO. The oxide is sufficiently porous to allow the reaction $Mn_3O_4 + CO = 3MnO + CO_2$ to proceed within the particles of oxide. Molten carbide (predominantly Mn_7C_3) is formed at points of contact by the reaction $7MnO + 10C = Mn_7C_3 + CO$. The carbide spreads over the surface of the particle and dissolves carbon which continues the reduction at the MnO carbide interface. An idealized model is shown diagrammatically in Fig. 2.

During the first stage of reaction, the CO diffuses into the particle and the chemical reaction is distributed throughout. This can be observed easily because of the development of the characteristic green coloration of MnO within the particle. The concentration of CO within the particle decreases from the outside towards the inside giving a profile as shown in the figure. The rate of reaction is strongly influenced by the local CO concentration giving higher rates at the outside of the pellet than near the center. Thus the Mn_3O_4 is completely converted to MnO at the outer surface sooner than anywhere else in the pellet. The interface then recedes towards the center.

The reaction sequence is somewhat more complex than is indicated in Fig. 2 because MnO is a nonstoichiometric oxide (Hed and Tannhauser[19]). At temperatures at which the reduction takes place, Mn_3O_4 converts to MnO having a metal deficiency of about 8 pct. This deficiency appears as metal vacancies in the MnO lattice. Before metallic Mn can nucleate from the lattice, the concentration of vacancies must be reduced to zero and it is not until then that the first stage of reduction in the model is complete. The vacancies are fairly mobile in the lattice and they provide a diffusional path for the reductant in nonporous oxide. However, the material discussed here is sufficiently porous for adequate supply of gaseous reductant and the transition from Mn_3O_4 through nonstoichiometric MnO to the stoichiometric oxide is ignored.

The impervious core in the second stage results from the very low value of K for the reaction $MnO + CO = Mn + CO_2$. Under most practical conditions, this reaction can be neglected entirely and the second stage proceeds according to the reaction $7MnO + 10C = Mn_7C_3 + 7CO$. Since the solid carbon cannot diffuse in oxide, all the reaction is localized at the MnO-Mn_7C_3 interface and the CO produced as a product of the reaction is available to diffuse through the MnO layer to continue the first-stage process further inside the pellet. The carbon is transported to the reaction interface by diffusion through the molten Mn_7C_3 layer either as dissolved carbon or as the metal carbide.

During the transition stage, both interfaces are present in the pellet. These interfaces appear simultaneously at the end of the first stage and the Mn_3O_4/MnO interface moves much more quickly than the MnO/Mn_7C_3 interface. The transition stage ends when the inner interface reaches the center of the pellet and reduction of Mn_2O_4 is complete.

The model as it is described above is an idealization

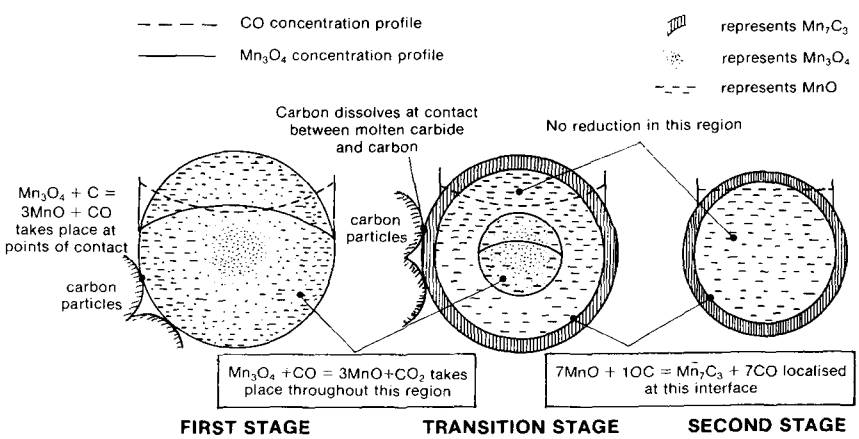

Fig. 2—Idealized model for the reduction of Mn_3O_4.

of the reduction mechanism for commercial manganese ores that are used for the production of ferromanganese. In particular we have neglected at least two features which are known to be significant: nucleation of metal does occur in the interior of a particle and the nonmetallic oxides present form a slag in which MnO is soluble and from which it is reduced to metal. The interior nucleation is probably due to the initial nucleation of iron from Wustite in the particle followed by dissolution of carbon and growth of the nuclei. The model should therefore be regarded as a useful simplification for data analysis. It has the merit of incorporating the two dominating processes, namely, the distribution of the first stage of the reaction throughout the porous oxide and the localization of the metallization reaction at the oxide-carbide interface.

In addition, both the iron and manganese oxides are reduced but for the purpose of our analysis, no distinction is made between them.

First Stage

The mathematical development for this stage is identical to that given by Ishida and Wen[12] for the single stage porous-core reaction and only their results which are essential for our later development are given here. The usual quasistationary assumption is made throughout so that changes in the position of the interface take place very much more slowly than the development of the concentration profiles in the particle. We have also assumed that CO and CO_2 are the only gaseous species in the interior of the particle. The rate of the reaction $Mn_3O_4 + CO = 3MnO + CO_2$ was assumed to be modelled by

$$R = s\rho kC(y_{co} - y_{co_2}/K) \qquad [17]$$

so that the overall (constant) rate of reaction during this stage is given by

$$\bar{R} = \eta_1 \frac{4}{3}\pi r_o^3 \rho skC\,(y_{co,b} - y_{co_2,b}/K) \qquad [18]$$

η_1, is the effectiveness factor

$$\eta_1 = \frac{3}{\phi^2\theta_1}(\phi \coth \phi - 1) \qquad [19]$$

which accounts for the internal diffusion and chemical reaction and θ_1 is the factor which accounts for external resistance

$$\theta_1 = 1 + (\phi \coth \phi - 1)/N_{sh} \qquad [20]$$

The time at which the first stage ends is

$$t_1 = \frac{C_s^o \theta_1}{\rho skC\,(y_{co,b} - y_{co_2,b}/K)} \qquad [21]$$

The unreacted solid concentration profile at the end of the first stage is given by

$$\frac{C_s^1}{C_s^o} = 1 - \frac{\sinh(\phi\xi)}{\xi \sinh \phi} \qquad [22]$$

and the fractional conversion at the end of stage one by

$$X_1 = \eta_1 \theta_1 f_1 \qquad [23]$$

Fractional conversion is defined as the loss in mass at any stage divided by the loss in mass after all reactions are complete. f_1 is the fractional conversion that would be obtained if only the first reaction went to completion throughout the particle.

The Transition Stage

i. The Movement of the Inner Interface. The transition stage starts when the first stage reduction is complete at the outer surface of the particle where the second stage reaction starts. Since the reductant (carbon) for the second stage reaction does not diffuse into the product of the first stage reaction (MnO), the second stage reaction proceeds with a shrinking impervious core. The porous core containing Mn_3O_4 and MnO shrinks steadily with an interface defined at the radius at which Mn_3O_4 is reduced to zero. The transition stage ends when the inner interface reaches the center of the particle and the Mn_3O_4 has been completely reduced to MnO. This marks the commencement of the second stage which proceeds until all the MnO has been completely reduced.

In the inner core the differential mass balance for CO is

$$\frac{1}{r^2}\frac{d}{dr}\left(r^2\frac{dy}{dr}\right) = \frac{s\rho k}{D_e'}(y - (1 - y)/K) \qquad [24]$$

with boundary conditions

BC1: $|y| < \infty$ at $r = 0$

BC2: $y = \bar{y}$ at $r = \bar{r}$

where the overbar represents conditions at the inner interface.

In the MnO layer, no chemical reaction takes place so that

$$\frac{1}{r^2}\frac{d}{dr}\left(r^2\frac{dy}{dr}\right) = 0 \qquad [25]$$

must be solved with BC2 and

BC3: $y = \bar{\bar{y}}$ at $r = \bar{\bar{r}}$

at the outer interface. $\bar{\bar{y}}$ is the mole fraction of CO generated at the outer interface.

In addition there must be equality of flux on either side of the inner interface so that

$$\text{BC4: } D_e \left.\frac{dy}{dr}\right|_{r=\bar{r}+} = D_e' \left.\frac{dy}{dr}\right|_{r=\bar{r}-}$$

After changing the variables to $x = y - 1/(1 + K)$ and $\xi = r/r_o$ the solution of Eqs. [24] and [25] with BC1, BC2, BC3 and BC4 gives the ratio of reductant concentration at the two interfaces as

$$\frac{\bar{x}}{\bar{\bar{x}}} = \frac{1}{1 + \frac{D_e'}{D_e}(1 - \bar{\xi}/\bar{\bar{\xi}})(\phi\bar{\xi}\coth(\phi\bar{\xi}) - 1)} = \frac{1}{\theta_2} \qquad [26]$$

The change of concentration Mn_3O_4 within the inner core is given by

$$\frac{dC_s}{dt} = -s\rho kC\,(y - (1 - y)K) \qquad [27]$$

The concentration profile for unreduced Mn_3O_4 in the porous core is found by the integration of [27] with the initial condition $C_s = C_s^1$ at $t = t_1$. The solution is

$$C_s = C_s^o\left(1 - \frac{\bar{\xi}\sinh(\phi\xi)}{\xi\sinh(\phi\bar{\xi})}\right) \qquad [28]$$

The rate at which the inner interface moves is given by Eq. [4],

$$\begin{aligned} R(\bar{r}) &= s\rho kC\,(\bar{y} - (1 - \bar{y})/K) \\ &= s\rho kC\bar{x}\frac{K + 1}{K} \\ &= s\rho kC\frac{K + 1}{K}\frac{\bar{\bar{x}}}{\theta_2} \end{aligned} \qquad [29]$$

Differentiating Eq. [28] and substituting in Eq. [4] gives

$$\frac{d\bar{\xi}}{dt} = -\frac{\bar{\xi}s\rho kC\,(K + 1)\bar{\bar{x}}}{KC_s^o\theta_2(\phi\bar{\xi}\coth(\phi\bar{\xi}) - 1)} \qquad [30]$$

for the rate of movement of the inner interface.

Unlike Eq. [11], Eq. [30] cannot be integrated directly because $\bar{\xi}$, and therefore θ_2, is a function of time and consequently the variables do not separate. Equation [30] must be integrated simultaneously with a similar differential equation for the position of the outer interface. Such an equation is developed in the next section.

ii. The Movement of the Outer Interface. The reaction at the outer interface is $7MnO + 10\,C = Mn_7C_3 + 7CO$. The rate of this reaction is constant provided that sufficient carbon is present to saturate the carbide layer on the outside of the particle. The equilibrium partial pressure for this reaction is larger than 1 atm and the mole fraction of the CO at the outer interface may be taken as that in the bulk gas phase.

Equation [16] gives

$$\frac{d\bar{\xi}}{dt} = -\frac{R_2}{r_oC_m^o} \qquad [31]$$

where C_m^o is the concentration of MnO after complete conversion of Mn_3O_4 to MnO. The stoichiometry of the reaction $Mn_3O_4 + CO = 3MnO + CO_2$ indicates that $C_m^o = 3C_s^o$. R_2 is evaluated at the interface between the metal layer and MnO and is the rate of the reaction $7MnO + 10C = Mn_7C_3 + 7CO$ per unit surface area of interface. Integrating [31] gives an explicit expression for the position of the outer interface at time t

$$\bar{\xi} = 1 - \frac{R_2}{3C_s^or_o}(t - t_1) \qquad [32]$$

Equation [32] can be used with [26] to solve [30] numerically which is a very simple procedure.

The fractional conversion is determined entirely by the position of the two interfaces. During the transition stage

$$\begin{aligned} X = 1 &- f_1\bar{\xi}^3 + \frac{3f_1\bar{\xi}}{4\phi^2}\,(\phi\bar{\xi}\coth(\phi\bar{\xi}) - 1) \\ &- (1 - f_1)\bar{\bar{\xi}}^3 \end{aligned} \qquad [33]$$

The Second Stage

During the second stage the outer interface position is given by [32] and the fractional conversion by

$$X = 1 - (1 - f_1)\bar{\bar{\xi}}^3 \qquad [34]$$

The time to complete conversion is given by

$$T = 3C_s^or_o/R_2 + t_1 \qquad [35]$$

after setting $\bar{\bar{\xi}} = 0$ in Eq. [32].

It is convenient to define a dimensionless time $\tau = t/T$ and a dimensionless ratio for the two reaction rates.

$$\Omega = \frac{3r_os\rho kC\,(y_{co,b} - y_{co_2,b}/K)}{R_2} \qquad [36]$$

Then the time to complete reaction is given by $\tau = 1$ and the time at the end of stage 1 by

$$\tau_1 = \theta_1/(\theta_1 + \Omega) \qquad [37]$$

Equation [30] becomes

$$\frac{d\bar{\xi}}{d\tau} = -\frac{\bar{\xi}(\Omega + \theta_1)}{\theta_2(\phi\bar{\xi}\coth(\phi\bar{\xi}) - 1)} \qquad [38]$$

and [32] becomes

$$\bar{\bar{\xi}} = 1 - (1 + \theta_1/\Omega)(\tau - \tau_1) \qquad [39]$$

The above relationships indicate that the progress of the reduction process is completely defined by five groups: the dimensionless time taken for the complete conversion of MnO as a shrinking core, $3r_oC_s^o/R_2$, the diffusion parameter ϕ for the first reaction, the dimensionless time constant for the first reaction at bulk gas conditions $C_s^o/s\rho kC\,(y_{co,b} - y_{co_2,b}/K)$, the ratio of diffusivities in the Mn_3O_4 and MnO layers D_e'/D_e and the Sherwood number for mass transfer across the gas layers on the outside of the pellet.

The transition stage does not occur if the surface reaction for the second stage reaction is faster than the first-stage reaction when the two interfaces do not separate. The second stage is then controlled by the rate of the first stage reaction. A precise condition for the appearance of the transition stage is developed in the appendix and is given by

$$\frac{\Omega}{\phi\coth\phi - 1} > 1 \qquad [40]$$

Such a criterion is easily checked.

EXPERIMENTAL

The rate of reduction was determined in a Stanton Thermogravimetric Balance Model HT-M (sensitivity = 0.1 mg). 2.5 g of preheated ore with 0.5 g of finely ground graphite were brought rapidly to temperature and the mass loss recorded. The furnace was flushed continuously with argon. The composition of the ore is given in Table I.

The experimental data are plotted as percentage reduction against time in Figs. 3, 4 and 5. The time axis is scaled by the time to reach complete conversion. That scaling reduced all the experimental data to a single line within the range of experimental precision. The data

Table I. Composition of the Ore (Wt Pct)

MnO	48.77	K_2O	0.34
CaO	12.70	P_2O_5	0.24
Fe_2O_3	6.37	Cr_2O_3	0.31
SiO_2	5.09	Al_2O_3	0.20
MgO	3.78	CO_2	14.88
H_2O	0.65	Total Mn	37.2 pct

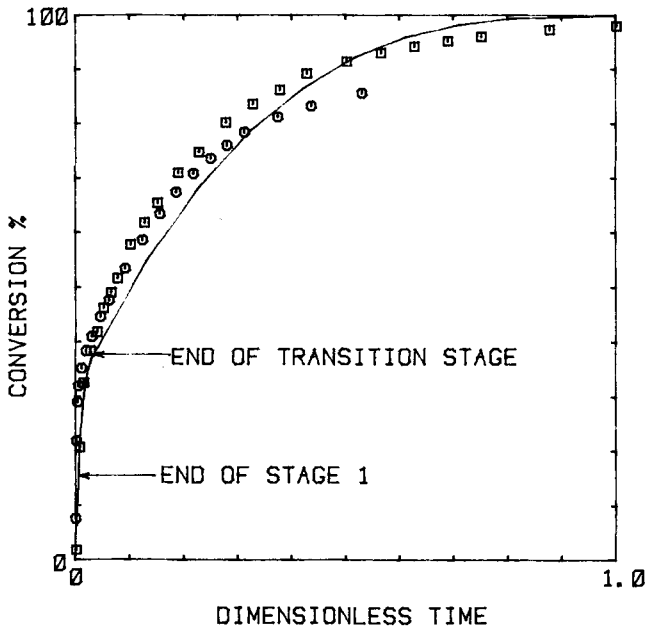

Fig. 3—Experimental data compared with model prediction for particles of commercial manganese ore of size +297 μm to 420 μm. ⊡ Experimental data at 1350 °C and time to complete conversion = 6 × 10³s. ⊙ Experimental data at 1250 °C and time to complete conversion = 24 × 10³s. —Model prediction with Ω = 150 and Φ = 5.

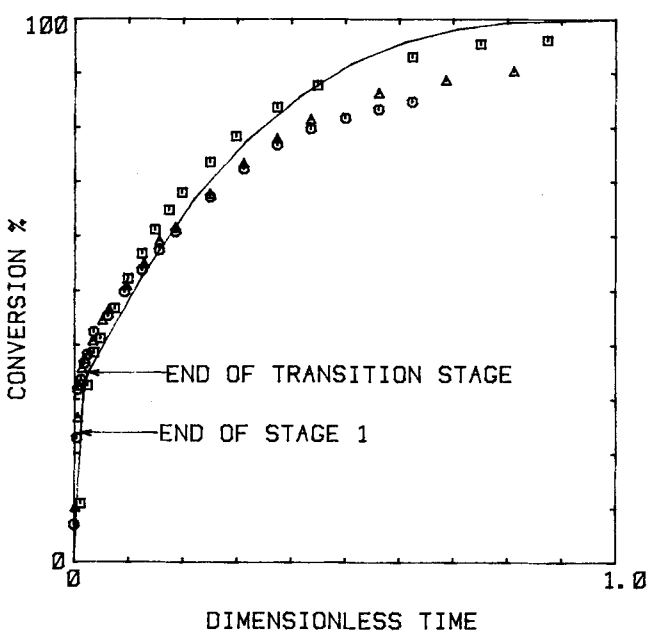

Fig. 4—Experimental data compared with model prediction for particles of commercial manganese ore of size + 149 μm to 210 μm. ⊡ Experimental data at 1350 °C and time to complete conversion = 3 × 10³s. ⊙ △ Experimental data at 1250 °C and time to complete conversion = 12 × 10³s. —Model prediction with Ω = 75 and Φ = 2.5.

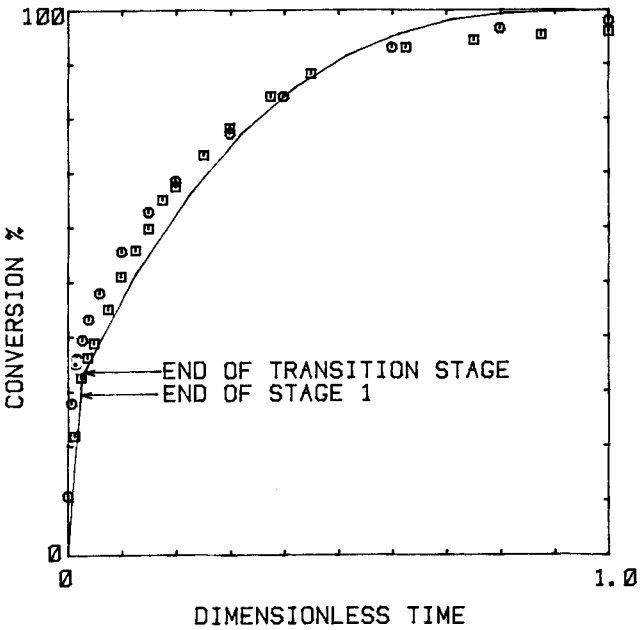

Fig. 5—Experimental data compare with model prediction for particles of commercial manganese ore of size +74 μm to 105 μm. ⊡ Experimental data at 1350 °C and time to complete conversion = 3 × 10³s. ⊙ Experimental data at 1250 °C and time to complete conversion = 9 × 10³s. —Model prediction with Ω = 37.5 and Φ = 1.25.

have been separated in the figures on the basis of the particle size.

The model predictions from Eqs. [23], [33] and [34] were plotted on the figures to demonstrate the usefulness of the two-stage model as a description of the reduction process. The parameters ϕ, Ω and T were chosen to obtain a satisfactory fit to the data.

In all the experiments, the time to reach the end of the transition stage was a very small fraction of the total reaction time. Thus Eq. [35] would indicate that the time to complete conversion should vary in proportion to the particle size. The data support this conclusion except in the smallest size.

The two parameters ϕ and Ω varied almost exactly in proportion to the mean particle size as required by Eqs. [7] and [36] although the model was insensitive to the precise values for these parameters.

CONCLUSION

1) A new exact Eq. [4] is derived for the rate of movement of a topochemical interface in a reacting solid when the core is porous.

2) The new equation is consistent with the description normally used for impervious core reactions.

3) The model can be extended to describe the gas-solid reaction schemes with multiple stages of reactions that are often encountered in practice.

4) The usefulness of the model is demonstrated by using it to provide a quantitative description of the reduction of a commercial manganese ore.

5) A complete description of the reduction of manganese oxide will require the incorporation of a model of the random nucleation of metal droplets in the interior of the particle. The model used here should be

regarded only as a useful working approximation and the agreement between the experimental data and the model predictions should not be taken as confirmation that the mechanism modelled is precisely the one that is operative in the reduction of manganese oxides.

APPENDIX

General Conditions for the Existence of a Transition Stage

A transition stage occurs only if the inner interface moves more rapidly than the outer. Thus a condition for the existence of a transition stage is

$$-\frac{d\bar{\xi}}{d\tau} > -\frac{d\bar{\bar{\xi}}}{d\tau} \text{ at } \bar{\xi} = \bar{\bar{\xi}} = 1 \qquad [A1]$$

Using the Eqs. [38] and [39] this gives

$$\frac{\Omega + \theta_1}{(\phi \coth \phi - 1} > \frac{\Omega + \theta_1}{\Omega} \qquad [A2]$$

or

$$\frac{\Omega}{\phi \coth \phi - 1} > 1$$

LIST OF SYMBOLS

C	total molar concentration of gas, mol m^{-3}
C_s	concentration of solid reactant, mol m^{-3}
C_s^o	concentration of solid reactant initially present, mol m^{-3}
D_e	effective diffusivity, $m^2 s^{-1}$
k	specific rate constant, ms^{-1}
k_g	mass transfer coefficient, ms^{-1}
K	equilibrium constant
N_{Sh}	Sherwood number for mass transfer through external gas layer. kg r_o/D_e
P	partial pressure, Nm^{-2}
r	radius, m
r_c	radius of core, m
r_o	outer radius of pellet, m
R	reaction rate, mol s^{-1} m^{-3}
R_2	rate of reaction between MnO and Mn_7C_3 on the surface of the impervious core, mol s^{-1} m^{-2}
s	pore surface area per unit mass of particle, m^2 kg^{-1}
t	time to complete conversion
t_1	time to end of stage 1, s
T	time to complete conversion, s
X	fractional conversion
x	$y - 1/(1 + K)$
$\bar{x}$	value of x at the inner interface
$\bar{\bar{x}}$	value of x at the outer interface
y	mole fraction in gas phase
η_1	effectiveness factor (Eq. [19])
$\theta\ \theta_1\ \theta_2$	factors for external resistances defined in Eqs. [6], [20] and [26]
ϕ	defined in Eq. [7]
κ	specific rate constant for reaction on surface of impervious core ms^{-1}
ξ	r/r_o
$\bar{\xi}$	r_c/r_o
$\bar{\bar{\xi}}$	r/r_o at the outer interface
ρ	bulk density of particle, kg m^{-3}

Subscripts

b	bulk gas phase exterior to particle
c	conditions at the core interface
s	solid phase
A,B,C,D	indicated molecular species

REFERENCES

1. R. H. Spitzer, F. S. Manning, and W. O. Philbrook: *Trans. TMS-AIME*, 1968, vol. 242, pp. 618–25.
2. M. Ishida and C. Y. Wen: *IEC Process Des. Dev.*, 1971, vol. 10, pp. 164–71.
3. J. Yagi, R. Takahashi, and Y. Omori: *Sci. Rep. Res. Inst. Tohoku Univ.*, 1971, vol. 23A, no. 1, pp. 31–47.
4. J. Szekely, J. W. Evans, and H. Y. Sohn: *Gas-Solid Reactions*, Academic Press, 1976.
5. R. H. Tien and E. T. Turkdogan: *Met. Trans.*, 1972, vol. 3, pp. 2039–48.
6. V. B. Mantri, A. N. Gokarn, and L. K. Doraiswamy: *Chem. Eng. Sci.*, 1976, vol. 31, pp. 779–85.
7. R. H. Spitzer, F. S. Manning, and W. O. Philbrook: *Trans. TMS-AIME*, 1966, vol. 236, pp. 1715–24.
8. D. Papanastassiou and G. Bitsianes: *Met. Trans.*, 1973, vol. 4, pp. 477–86.
9. G. Nabi and W. K. Lu: *Trans. TMS-AIME*, 1968, vol. 242, pp. 2471–77.
10. E. T. Turkdogan and J. V. Vinters: *Met. Trans.*, 1971, vol. 2, pp. 3175–88.
11. R. Takahashi, J. Yagi, and U. Omori: *Sci. Rep. Res. Inst. Tohoku Univ.*, 1971, vol. 23A, pp. 9–30.
12. M. Ishida and C. Y. Wen: *AIChEJ*, 1968, vol. 14, pp. 311–17.
13. H. O. Lien, A. E. El-Mehairy, and H. U. Ross: *J. Iron Steel Inst.*, 1971, pp. 541–45.
14. L. von Bogdandy and H. J. Engell: *The Reduction of Iron Ores*, Springer-Verlag, 1971.
15. N. A. Barcza, P. R. Jochens, and D. D. Howat: *Electr. Furn. Proc.*, 1971, vol. 29, pp. 88–93.
16. W. D. Grimsley, J. B. See, and R. P. King: *J. S. Afr. Inst. Min. Metall.*, 1977, vol. 78, pp. 51–62.
17. A. M. Ginstling and B. I. Brounshtein: *J. Appl. Chem. USSR*, 1950, vol. 23, pp. 1237–1338.
18. W. C. Scrivner and E. S. Manning: *AIChEJ*, 1970, vol. 16, pp. 326–29.
19. A. Z. Hed and D. S. Tannhauser: *J. Electrochem. Soc.*, 1967, vol. 114, pp. 314–18.